Title
Triple Inverse Sandwich versus End-On Diazenido: Bonding Motifs across a Series of Rhenium—Lanthanide and —Actinide Complexes

Journal
Inorganic Chemistry, 63(16)

ISSN
0020-1669

Authors
Ouellette, Erik T
Brackbill, I Joseph
Kynman, Amy E
et al.

Publication Date
2024-04-22

DOI
10.1021/acs.inorgchem.3c04248

Triple inverse sandwich versus end-on diazenido: bonding motifs across a series of rhenium-lanthanide and -actinide complexes

Erik T. Ouellette,[†,§] I. Joseph Brackbill,[†,§] Amy E. Kynman,[†,§] Stella Christodoulou,[‡] Laurent Maron,[‡] Robert G. Bergman,[†] John Arnold[†,§,*]

[†]*Department of Chemistry, University of California, Berkeley, California 94720, USA*
[§]*Chemical Sciences Division, Lawrence Berkeley National Laboratory, Berkeley, California 94720, USA*
[‡]*LPCNO, Université de Toulouse, INSA Toulouse, 135 Avenue de Rangueil, 31077 Toulouse, France*

*Email: arnold@berkeley.edu

Abstract

While synthesizing a series of rhenium-lanthanide triple inverse sandwich complexes, we unexpectedly uncovered evidence for rare examples of end-on lanthanide dinitrogen coordination for certain heavy lanthanide elements, as well as for uranium. We begin our report with the synthesis and characterization of a series of tri-rhenium triple inverse sandwich complexes with the early lanthanides, Ln[(μ-η^5:η^5-Cp)Re(BDI)]$_3$(THF) (**1-Ln**, Ln = La, Ce, Pr, Nd, Sm; Cp = cyclopentadienide, BDI = *N*,*N*′-bis(2,6-diisopropylphenyl)-3,5-dimethyl-*β*-diketiminate). However, as we moved across the lanthanide series, we ran into an unexpected result for gadolinium in which we structurally characterized two products for gadolinium, namely **1-Gd** (analogous to **1-Ln**) and a diazenido di-rhenium double inverse sandwich complex Gd[(μ-η^1:η^1-N_2)Re(η^5-Cp)(BDI)][(μ-η^5:η^5-Cp)Re(BDI)]$_2$(THF)$_2$ (**2-Gd**). Evidence for analogs of **2-Gd** was spectroscopically observed for other heavy lanthanides (**2-Ln**, Ln = Tb, Dy, Er), and, in the case of **2-Er**, structurally authenticated. These complexes represent the first observed examples of heterobimetallic end-on lanthanide dinitrogen coordination. Density functional theory (DFT) calculations were utilized to probe relevant bonding interactions and reveal energetic differences between both experimental and putative **1-Ln** and **2-Ln** complexes. We also present additional examples of novel end-on heterobimetallic lanthanide- and actinide-diazenido moieties in erbium-rhenium complex (η^8-COT)Er[(μ-η^1:η^1-N_2)Re(η^5-Cp)(BDI)](THF)(Et_2O) (**3-Er**) and uranium-rhenium complex [Na(2.2.2-cryptand)][(η^5-$C_5H_4SiMe_3$)$_3$U(μ-η^1:η^1-N_2)Re(η^5-Cp)(BDI)] (**4-U**). Finally, we expand the scope of rhenium inverse sandwich coordination by synthesizing divalent double inverse sandwich complex Yb[(μ-η^5:η^5-Cp)Re(BDI)]$_2$(THF)$_2$ (**5-Yb**), as well as base-free, homoleptic rhenium-rare earth triple inverse sandwich complex Y[(μ-η^5:η^5-Cp)Re(BDI)]$_3$ (**6-Y**).

Introduction

Despite a commonly held notion that the lanthanides are effectively identical in terms of chemical properties and reactivity, there is in fact a good deal of nuance to the diversity of these fifteen *f*-block congeners. For example, while the trivalent oxidation state still dominates the chemistry of the lanthanides, an increasing number of complexes isolated in the divalent[1–10] or tetravalent[11–21] oxidation states have been reported in recent years. Through rational ligand choice and molecular design, lanthanide complexes have recently been developed for a wide range of chemical applications, including molecular magnetism,[22–33] luminescence and optics,[34–38] and catalysis.[39–47] Even when considering only the trivalent state, the

lanthanides display a broad spectrum of chemical traits, particularly between the early (lighter) and late (heavier) elements. A commonly discussed concept, known as the "gadolinium break," has been used as somewhat of a catch-all for describing inconsistencies in chemical and physical properties across the lanthanide series.[48,49] Some of these disparities are specific to gadolinium(III), often posited as a result of its half-filled 4*f* shell.[49] Other deviations, such as preferred coordination numbers and trends in chemical reactivity, encompass the full set of lanthanides, with gadolinium often acting as a figurative breaking point.[50–55] In other cases, there appears to be no significant deviation in properties and thus no evidence of a gadolinium break,[48,56,57] highlighting that deviations in lanthanide properties should be analyzed more by the specific application rather than in the context of misleading, all-encompassing, concepts such as a "gadolinium break." In any case, correlating observed trends in lanthanide reactivity with physical properties is crucial to advancing our understanding of molecular lanthanide chemistry for future applications.

Recent progress has been made in the synthesis of multimetallic and heterometallic lanthanide complexes.[58–64] Investigating the interactions between lanthanides and other metals, either directly or through bridging ligands, should improve our understanding of fundamental lanthanide bonding properties, particularly when it is possible to compare analogous structures made with a series of lanthanide ions. Our group reported the isolation of a rhenium-uranium triple inverse sandwich complex, U[(μ-η^5:η^5-Cp)Re(BDI)]$_3$(L), which was synthesized via a modular approach utilizing a Na[Re(η^5-Cp)(BDI)] metalate for the installation of three rhenium(I) metalloligands onto the U^{3+} ion.[65] Given that result, we were curious about whether an analogous synthetic strategy could be applied toward the lanthanides, a set of similarly large electropositive *f*-block metals. A number of inverse sandwich complexes of the lanthanides have been reported,[2,66–96] but examples of heterobimetallic inverse sandwich bonding between a lanthanide and another metal are exceedingly rare.[97,98] Here, we report the synthesis of a series of rhenium triple inverse sandwich complexes involving early lanthanides, as well as the discovery of an unexpected divergence in reactivity between early and late lanthanides wherein we obtain evidence for novel end-on/end-on rhenium-lanthanide diazenido complexes involving gadolinium and heavier lanthanides. We investigate this series of unique complexes, as well as related heterobimetallic rhenium-lanthanide and -actinide diazenido species, through a variety of synthetic and computational investigations.

Results and Discussion

Synthesis of Early Lanthanide-Rhenium Triple Inverse Sandwich Complexes

Inspired by our previous synthetic route to U[(μ-η^5:η^5-Cp)Re(BDI)]$_3$(L), we began our investigations with the lanthanide series by attempting salt elimination reactions between Na[Re(η^5-Cp)(BDI)] and lanthanide(III) chlorides. Our early results were mixed: the insolubility of $LnCl_3$ necessitated long reaction times that led to deleterious reactivity,[99] and we had difficulty isolating clean products. However, turning to the more soluble lanthanide(III) iodide adducts, $LnI_3(L)_x$ (L = Et_2O, THF), made a marked difference. These reactions, run in THF, led to dark red solutions and the crude products were easily extracted into hexane, from which dark red crystals were isolated in moderate yields. For the early lanthanides, the products were identified as a series of rhenium-lanthanide triple inverse sandwich complexes, Ln[(μ-η^5:η^5-Cp)Re(BDI)]$_3$(THF) (Ln = La, Ce, Pr, Nd, Sm) (Scheme 1).

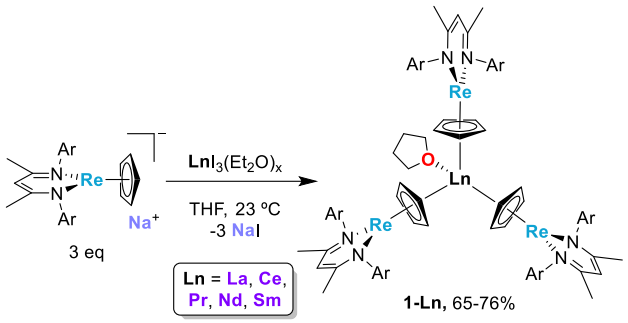

Scheme 1. Synthesis of triple inverse sandwich complexes **1-Ln** (Ln = La, Ce, Pr, Nd, Sm).

Despite the paramagnetic nature of these complexes (other than **1-La**), the ^{1}H and ^{13}C NMR resonances attributable to the [(μ-η^5:η^5-Cp)Re(BDI)] fragments were relatively sharp and located primarily within the diamagnetic region (Figures S1–S10), though certain resonances for the Cp protons (bound directly to the paramagnetic Ln(III) centers) were found to be slightly broadened (in **1-Pr**) and/or shifted either upfield (δ = –1.17 ppm in **1-Nd**) or downfield (δ = 6.75 ppm in **1-Sm**). The resonances for the bound THF protons are influenced more significantly by the paramagnetism, as they are broadened significantly and found farther upfield in **1-Ce**, **1-Nd**, **1-Sm** and are unobservable in **1-Pr**. The spectra also confirm C_{3v} solution geometries for these five complexes, with three symmetrically equivalent [(μ-η^5:η^5-Cp)Re(BDI)] metalloligands. Given the sharp resonances and presumed absence of notable unpaired spin density around rhenium, we believe these complexes are best described as three Re(I) metalloligands surrounding a Ln^{3+} ion, corroborating the electronic structure observed in U[(μ-η^5:η^5-Cp)Re(BDI)]$_3$(L).[100]

The solid-state structures for **1-Ln** (Ln = La Ce, Pr, Nd, Sm, and Gd – see below for discussion of **1-Gd** synthesis) were determined through X-ray crystallography (Figures 1 and S32-36). Single crystals were grown from either hexane or pentane, though we found it was also necessary in certain instances to add a drop of THF to the recrystallization vial in order to spur growth of high-quality crystals, which is consistent with our previous conclusion that Lewis bases act to stabilize and facilitate crystallization of U[(μ-η^5:η^5-Cp)Re(BDI)]$_3$(L).[100] The average Ln–Cp bond distances, measured either as Ln–Cp(C) or Ln–Cp(centroid) distances, decrease across the lanthanide series from **1-La** to **1-Gd** as expected with the corresponding decrease in ionic radius (Figure 2, Table S17). These distances, as well as the Ln–O bond distances and overall geometry, are generally consistent with the analogous measurements in reported Ln(η^5-Cp)$_3$(THF) complexes (Table S18).[101–106] However, the average Re–Cp distances, which do not deviate significantly across the **1-Ln** series (mean Re–Cp(C) distances range from 2.148 to 2.158 Å), are contracted relative to the Na[Re(η^5-Cp)(BDI)] starting material (Re–Cp(C) = 2.153(6) to 2.211(4) Å). This shortening of the Re–Cp distance, measured either as Re–Cp(C) or Re–Cp(cent) distances, is consistent with that observed in related U[(μ-η^5:η^5-Cp)Re(BDI)]$_3$(L) (Figure 2), with the degree of shortening nearly indistinguishable between the **1-Ln** (Ln = La, Ce, Pr, Nd, Sm, Gd) complexes and the analogous uranium structure; the longest Re–Cp(cent) distance in **1-Ln** is found in **1-Pr** at 1.773(5) Å and the shortest in **1-Sm** at 1.761(2) Å, whereas in the uranium analog it is 1.763(4) Å. In the case of uranium, the shortened Re–Cp distances were posited to occur due to a reduction in Coulombic repulsion in the Re–Cp internuclear region as the highly Lewis acidic uranium center pulls electron density toward itself.[65] An analogous effect is understandable for similarly Lewis acidic lanthanide ions. Lastly, the Re–N distances in **1-Ln**, which are again consistent across the series (ranging from 2.035(2) to 2.050(2) Å with a mean distance of 2.045 Å), are also slightly elongated relative to the same bonds in Na[Re(η^5-Cp)(BDI)] (2.031(3) Å)[107] but still consistent with our assignment of rhenium(I) fragments.

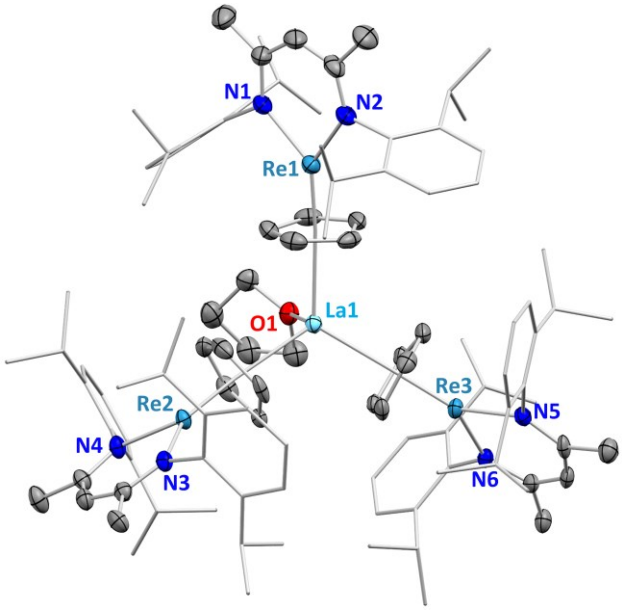

Figure 1. X-ray crystal structures of **1-La** shown with 50% probability ellipsoids. The BDI aryl groups are shown in wireframe, and hydrogen atoms and cocrystallized solvent molecules are omitted for clarity.

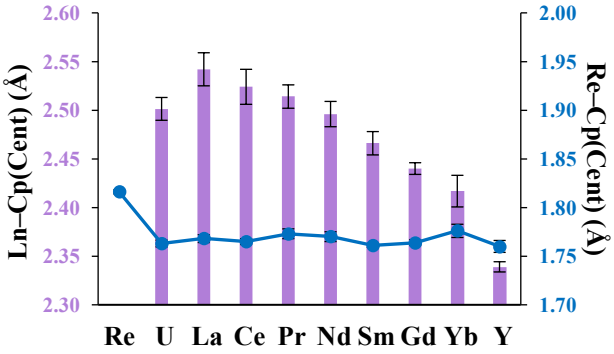

Figure 2. Plot of average metal to Cp centroid distances (Å) for **1-Ln** (Ln = La, Ce, Pr, Nd, Sm, Gd) compared to reference structures Na[Re(η^5-Cp)(BDI)] ("**Re**")[107] and U[(μ-η^5:η^5-Cp)Re(BDI)]$_3$(THF) ("**U**")[65] highlighting contraction of the Re–Cp bond in these inverse sandwich complexes. Additionally, comparable structures Yb[(μ-η^5:η^5-Cp)Re(BDI)]$_2$(THF)$_2$ (**5-Yb**) and Y[(μ-η^5:η^5-Cp)Re(BDI)]$_3$ (**6-Y**) are shown for further comparison with divalent ("**Yb**") and homoleptic ("**Y**") complexes (*vida infra*). Ln–Cp(Cent) distances represented by purple columns and Re–Cp(Cent) distances represented by a blue line plot.

To gain insight into the bonding of **1-Ln**, DFT calculations were carried out utilizing the B3PW91 functional,[108,109] given that this computational approach has been previously used to described the analogous uranium complex[65] (see SI for full computational details). To check for 4*f* orbital involvement, calculations were carried out with *f*-in-core relativistic effective core potentials (RECP), adapted to the 3+ oxidation state of the lanthanide.[110] This methodology has proven its ability to describe the geometry and bonding of a large number of lanthanide complexes.[111–114] Geometry optimizations were then carried out for the

complexes **1-La**, **1-Sm**, **1-Gd** and the putative **1-Dy**. Local minima were identified for all four triple inverse sandwich complexes, and the optimized geometries agree well with the crystallographic data (Tables S19-S20). The Ln–Cp(cent) distances are reproduced within 0.06 Å while the Re–Cp(cent) distances are within 0.02 Å. In the latter case, the Re–Cp(cent) distances are again similar across the series and relatively shortened (*vide supra*), as in the case of U[(μ-η^5:η^5-Cp)Re(BDI)]$_3$(L).[65] The lanthanide contraction is also reproduced computationally across the series. Additionally, the calculations suggest that lanthanide 4*f* orbitals do not contribute significantly to the bonding picture, with the largest contribution coming in **1-La** (2.0%) and decreasing in **1-Sm** (1.5%) and **1-Gd** (1.2%) (Table S21). In fact, the three highest molecular orbitals (HOMOs) are δ bonds involving 5*d* orbitals on Re, 5*d* orbitals on Ln and π* orbitals on the Cp ligands (Figure 3). Orbital analysis of the inverse sandwich bonds (M–Cp–Re) reveals a 50% metal and 50% Cp contribution to the bonds, the same distribution as was found in the analogous uranium analog.[65] However, the lanthanides contribute slightly less to the bonding picture than uranium, as we calculate a 20% Ln to 80% Re ratio for **1-Ln** (La, Sm, Gd) compared to a 25% to 75% ratio in U[(μ-η^5:η^5-Cp)Re(BDI)]$_3$(THF),[65] a result consistent with the current understanding that actinides can form more covalent bonds than the lanthanides.[115,116]

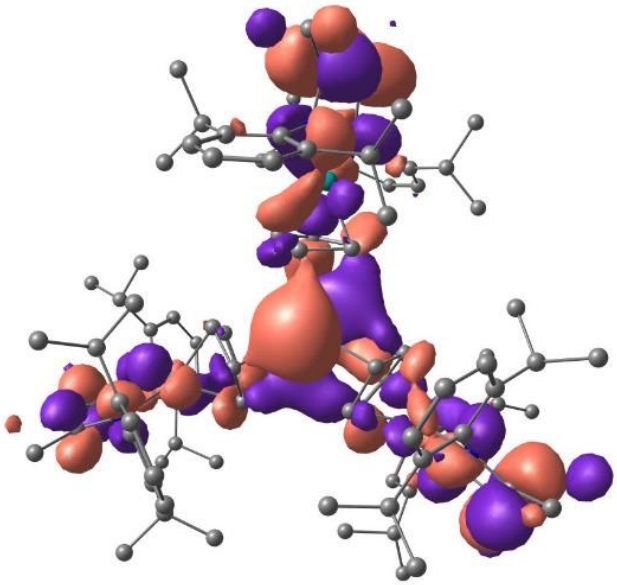

Figure 3. Rendering of the HOMO δ-bond for complex **1-Sm** (isosurface value of 0.03).

Diazenido Formation in Mid-to-Late Lanthanides

During our attempts to extend the triple inverse sandwich motif further across the lanthanide series, we were unable to cleanly isolate such complexes for any of the Ln^{3+} metals heavier than samarium. Reactions between Na[Re(η^5-Cp)(BDI)] and mid-to-late lanthanide(III) halides (Gd, Tb, Dy, Er) in THF led to dark red reaction mixtures, but after extracting the crude material into hexane or pentane, we had difficulty initiating crystallization of products. This was in contrast to the early lanthanides, which crystallized nicely from hexane, and indicated that we may be observing different reactivity as we move across the lanthanide series. Eventually, we were able to obtain small crops of crystals from hexane resulting from reactions between Na[Re(η^5-Cp)(BDI)] and either $GdCl_3$ or $GdI_3(Et_2O)_3$. ^{1}H NMR analysis of these crystals was not particularly informative, as the peaks were broadened and paramagnetically shifted, and

we were unable to confidently assign resonances. However, FT-IR measurements revealed an unexpected strong stretching frequency at 1715 cm^{-1} (Figure S24), which we postulated may be attributable to an N=N stretch similar to other heterobimetallic rhenium complexes we had previously synthesized.[117–119] We were able to recrystallize this material from pentane and XRD studies corroborated our suspicions, as we determined the product structure to be Gd[(μ-η^1:η^1-N_2)Re(η^5-Cp)(BDI)][(μ-η^5:η^5-Cp)Re(BDI)]$_2$(THF)$_2$ (**2-Gd**, Scheme 2, Figure 4), which contains dinitrogen incorporated from the reaction atmosphere. We obtained a second crop of crystals after concentrating the supernatant removed from the initial crop of **2-Gd,** for which FT-IR measurements did not contain any stretching frequency in the 1600–2000 cm^{-1} region, suggesting an absence of any diazenido N=N bonds (Figure S24). By recrystallizing this second crop from pentane, we were able to obtain another set of single crystals suitable for XRD, which this time revealed the product as Gd[(μ-η^5:η^5-Cp)Re(BDI)]$_3$(THF) (**1-Gd**), being isostructural with the **1-Ln** products discussed earlier (Figure 1).

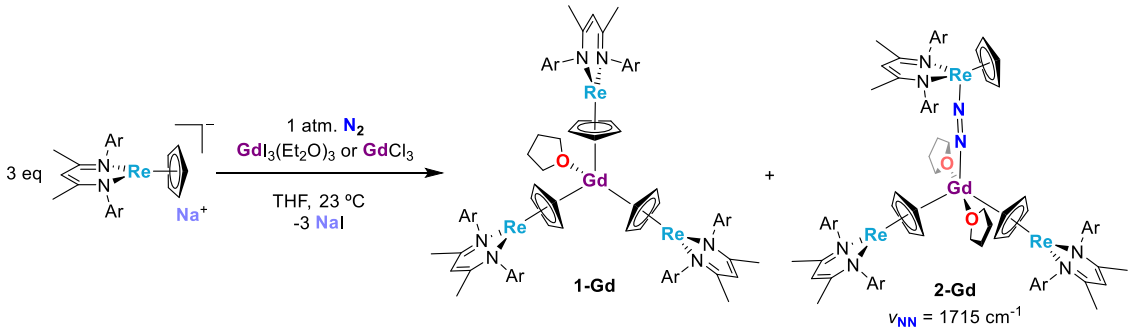

Scheme 2. Synthesis of both lanthanide-rhenium diazenido complex **2-Gd** and triple inverse sandwich complex **1-Gd**.

Formation of dinitrogen-incorporated **2-Gd** was unexpected given that these reactions were performed at room temperature and that end-on lanthanide dinitrogen bonding is highly unusual.[120–124] While we have significant evidence from prior studies that the Na[Re(η^5-Cp)(BDI)] metalate reversibly binds and activates dinitrogen in solution,[117–119,125] we typically only observe significant dinitrogen incorporation into resulting reaction products when performing reactions at low temperatures (ca. –78 ºC). Additionally, we had seen no evidence of any dinitrogen incorporation in reactions producing **1-Ln** (Ln = La, Ce, Pr, Nd Sm), and when we performed subsequent FT-IR measurements on newly synthesized crude products of those early lanthanide reactions, we still did not observe any stretching frequencies that could be attributed to N=N formation. As another control experiment, we also attempted a low-temperature reaction (–78 ºC) with $LaI_3(Et_2O)_3$ and again saw no evidence of dinitrogen incorporation in FT-IR spectra of the crude product mixture. These results suggested a specific change in the reactivity pattern as we move to gadolinium in the lanthanide series.

While the gadolinium diazenido **2-Gd** was our first direct evidence of N_2 incorporation with the middle lanthanides, we soon thereafter discovered similar N=N stretching frequencies in FT-IR spectra of crude product material from reactions between Na[Re(η^5-Cp)(BDI)] and $LnX_3(L)_x$ (Ln = Tb, Dy, Er; X = Cl, I). Each of these displayed strong stretching frequencies at 1713 to 1717 cm^{-1} (Figures S25-S27), strongly suggesting the formation of diazenido complexes analogous to **2-Gd** (Scheme 3). Unfortunately, despite efforts to promote formation of these diazenido complexes using low-temperature reaction conditions, we were unable to isolate clean product material due to the presence of known side products[99] as well as potential unidentifiable impurities; **2-Er** was the only other complex for which we could obtain a solid-state structure (Figure 4). While the FT-IR data corroborated the formation of diazenido species for

the late lanthanides (Er, Tb, Dy), we also performed reactions between Na[Re(η^5-Cp)(BDI)] and $LnX_3(L)_x$ (Ln = Tb, Dy, Er; X = Cl, I) under an atmosphere of argon in an attempt to generate triple inverse sandwich-type complexes for these heavy lanthanides. These attempts were unsuccessful, however, and led to intractable mixtures.

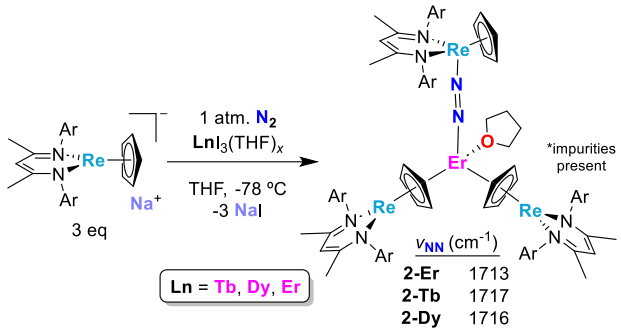

Scheme 3. Evidence for lanthanide-rhenium diazenido complexes **2-Ln** (Ln = Er, Tb, Dy). Complex **2-Er** was structurally authenticated and **2-Tb/2-Dy** are postulated based on their analogous IR stretching frequencies, though none could be isolated cleanly.

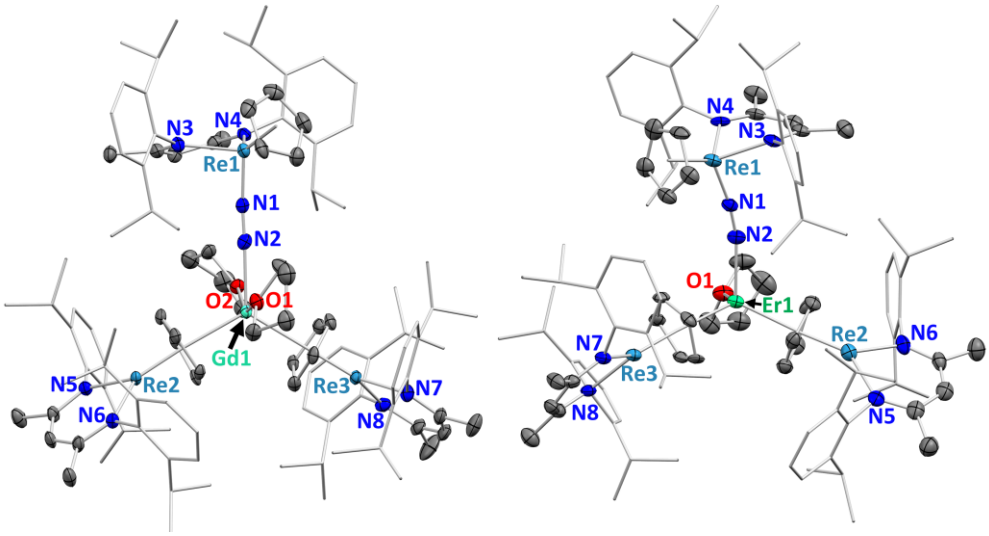

Figure 4. X-ray crystal structures of **2-Ln** (Ln = Gd (left), Er (right)) shown with 50% probability ellipsoids. The BDI aryl groups are shown in wireframe, and hydrogen atoms are omitted for clarity.

Similar to the computational investigation of **1-Ln**, geometry calculations were carried out for **2-Gd** and **2-Dy** and the putative complexes **2-La** and **2-Sm**, all of which were predicted to be stable (Tables S19 and S21). The putative dinitrogen insertion energy of complexes **1-Ln** to yield complexes **2-Ln** were computed and in all cases the formation of complexes **2-Ln** are found to be thermodynamically favored by 8 to 12 kcal mol^{-1}. Therefore, the lack of formation of complex **2-Ln** in all cases may be a kinetic problem. As for the bonding in **2-Ln**, the N–N distance in the complex is compatible with a doubly reduced N_2 which is corroborated by the nature of the HOMO-6 in complex **2-Dy** (Figure 5). In this MO, there is bonding overlap between a 5d orbital on Dy, the N_2 π^* orbital and a 5d orbital on Re.

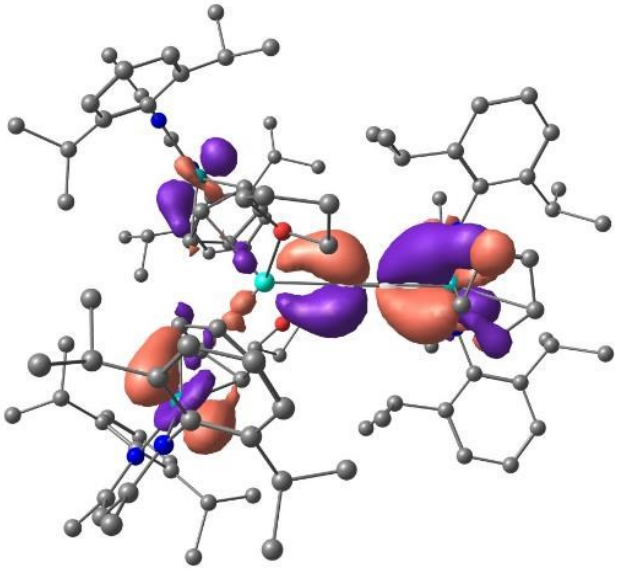

Figure 5. Rendering of the HOMO-6 orbital for complex **2-Dy** (isosurface value of 0.03).

The collective sum of experimental and computational investigations on the formation of **1-Ln** versus **2-Ln** suggest that there is a change in reactivity between the early lanthanides and the later lanthanides (from gadolinium on). While the early lanthanides react with Na[Re(η^5-Cp)(BDI)] by forming three inverse sandwich type bonds, adopting a common geometry reminiscent of $LnCp_3(L)$, the heavier lanthanides resist adopting the same configuration. Instead, these lanthanides prefer to form just two inverse sandwich type bonds with the [(η^5-Cp)Re(BDI)] metalloligand, with the third equivalent of rhenium bonding through a diazenido ligand to the lanthanide center. We postulate that the decrease in ionic radius moving from the early to late lanthanides, with the concurrent decrease in preferred coordination number, may be at the heart of our observed reactivity. As the ionic radii of Ln^{3+} ions decreases across the series, it may become less favorable sterically (and kinetically) to have three bulky [(η^5-Cp)Re(BDI)] metalloligands approach and react with the lanthanide ion center (as in **1-Ln**). Instead, the thermodynamically favorable diazenido-double inverse sandwich type structures (**2-Ln**) predominate for gadolinium and heavier lanthanides. Mechanistically, formation of the **2-Ln** complexes also requires the cooperation of the Na[Re(η^5-Cp)(BDI)] reagent to initially bind dinitrogen (as observed in prior studies[117–119,125]) before reacting with the lanthanide halide. Thus, mechanistic complications and concurrent formation of unproductive side products due to deleterious reactivity of the sensitive Na[Re(η^5-Cp)(BDI)] metalate* make it difficult to cleanly isolate **2-Ln** in good yields.

Synthesis of Comparable Lanthanide and Actinide Diazenido Complexes

Given the unexpected formation of a terminal diazenido fragment bound to a lanthanide in **2-Ln**, we were curious to determine whether reactions between Na[Re(η^5-Cp)(BDI)] and other late lanthanide(III) reagents would lead to inverse sandwich or diazenido type coordination of the rhenium metalloligand. Fortuitously, around this time we had also been experimenting with installing the [(η^5-Cp)Re(BDI)] ligand into a (Cp*)Ln(COT) (Cp* = $C_5Me_5^{1-}$, COT = $C_8H_8^{2-}$) type architecture; we were interested in studying the impact replacing the Cp* ligand with a rhenium metalloligand would have on the magnetic properties of the molecules.[126,127] We began by attempting room-temperature reactions between Na[Re(η^5-Cp)(BDI)] and

(COT)ErCl(THF)$_x$ in THF. From these reactions, we obtained small dark red crystals of crude products following workup and crystallization from Et_2O. FT-IR measurements revealed a strong stretch at 1770 cm^{-1} [1] (Figure S28), an early indication that dinitrogen had been incorporated yet again. Recrystallization from Et_2O led to single crystals of X-ray quality, which revealed the structure to be (η^8-COT)Er[(μ-η^1:η^1-N_2)Re(η^5-Cp)(BDI)](THF)(Et_2O) (**3-Er**, Scheme 4, Figure 6), though we were unable to isolate analytically pure material suitable for elemental analysis. While the bridging diazenido product precluded us from being able to isolate the desired inverse sandwich erbium(III) complex for magnetic study, the observation of diazenido formation helped to reinforce the preferred bonding mode between the [(η^5-Cp)Re(BDI)] metalloligand and heavy lanthanide ions.

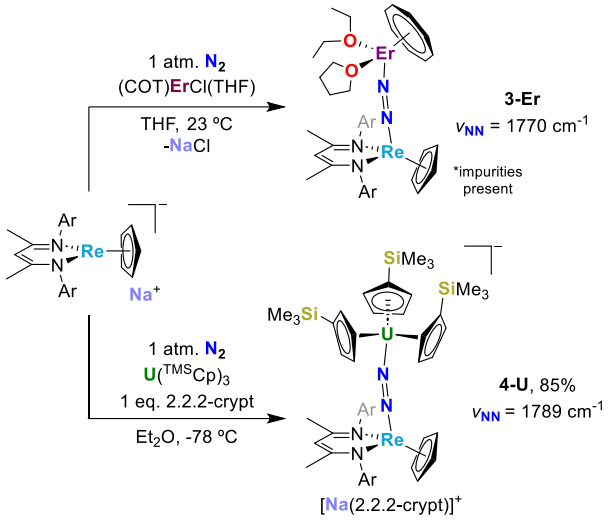

Scheme 4. Synthesis of lanthanide- and actinide-rhenium diazenido complexes **3-Er** and **4-U**.

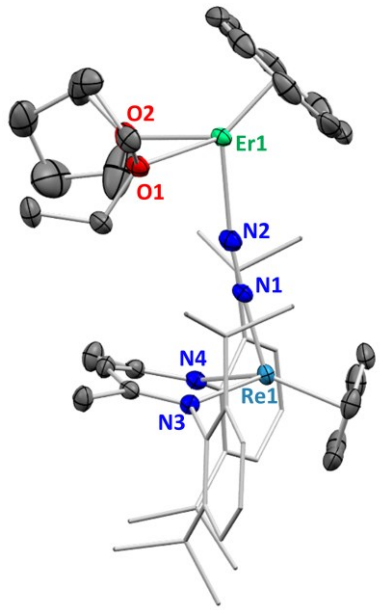

Figure 6. X-ray crystal structure of **3-Er** shown with 50% probability ellipsoids. The BDI aryl groups are shown in wireframe. Hydrogen atoms, a second molecular unit in the asymmetric unit, and cocrystallized Et_2O molecules are all omitted for clarity.

We also revisited our attempts to form a diazenido-type bond to uranium(III), considering that our initial report of a triple inverse sandwich complex had included no efforts to enforce diazenido bonding to uranium.[65] To favor N_2 binding by Na[Re(η^5-Cp)(BDI)], we attempted a low temperature reaction (–78 ºC) with UI_3(1,4-dioxane)$_{1.5}$; however, FT-IR spectra of the crude reaction material included no indication of diazenido formation. Our inability to form a diazenido in this case seems reasonable considering the large ionic radius of U^{3+} and its preference for higher coordination numbers.

We made a separate effort to form a uranium diazenido complex using another U^{3+} reagent, this time utilizing U(Cp^{TMS})$_3$ (Cp^{TMS} = $C_5H_4SiMe_3$),[128] which our group has previously used to bond to a variety of donor fragments.[129,130] At –78 ºC, we added a solution of Na[Re(η^5-Cp)(BDI)] to a solution containing both U(Cp^{TMS})$_3$ and [2.2.2-cryptand] in Et_2O, and from the reaction mixture we were eventually able to isolate dark red crystals of diazenido complex [Na(2.2.2-cryptand)][(Cp^{TMS})$_3$U(μ-η^1:η^1-N_2)Re(η^5-Cp)(BDI)] (**4-U**, Scheme 4) in good yield, allowing us to characterize it further. Despite the paramagnetic U^{3+} ion, we were able to observe sharp ^{1}H and ^{13}C NMR resonances for the product (Figures S14–S15). We also identified a clear N=N stretching frequency in the infrared spectrum at 1789 cm^{-1} (Figure S29), and X-ray diffraction allowed for determination of the full diazenido structure (Figure 7).

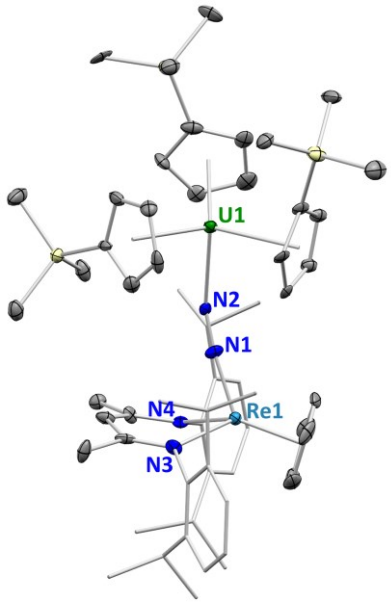

Figure 7. X-ray crystal structure of **4-U** shown with 50% probability ellipsoids. The BDI aryl groups are shown in wireframe. Hydrogen atoms, a second molecular unit in the asymmetric unit, Na[2.2.2-cryptand] counterion units, and cocrystallized Et_2O molecules are all omitted for clarity.

Lanthanide- and actinide-rhenium diazenido complexes **2-Ln**, **3-Er**, and **4-U** have fairly comparable diazenido geometries (Table 1). Most noteworthy are the N–N distances, which range from 1.16(2) Å for **4-U** to 1.193(8) Å for **2-Er** and are elongated relative to free N_2 (1.098 Å).[131] This lengthening of the N–N bond is corroborated by the observed stretching frequencies (1713–1789 cm^{-1}), which indicate significant bond activation relative to free N_2 (2359 cm^{-1}).[132] While the Re–N bond distances to the diazenido fragment are consistently ca. 1.8 Å in these four complexes, the Ln–N or U–N distances are specific to each metal and trend in accordance with their ionic radii, with the shortest bond measuring

2.179(6) Å for **2-Er** and the longest 2.448(9) Å for **4-U**. While not perfectly linear, the measured Re–N1–N2 and M–N2–N1 angles are all between 157° and 178°, indicating they are not particularly bent. Interestingly, **3-Er**, which contained two molecular units within the asymmetric unit of the triclinic cell, had fairly different diazenido angles for the two individual units, indicating that perhaps the angles in this particular complex are sensitive to crystal packing considerations. In any case, the general end-on/end-on coordination of these heterobimetallic diazenido complexes is clearly displayed in the solid-state structures.

These diazenido complexes are noteworthy given the rarity of end-on coordination of "N_2" fragments to lanthanide and actinide metals. Admittedly, the heavy-lifting in terms of dinitrogen binding and activation is likely accomplished by the Na[Re(η^5-Cp)(BDI)] starting material prior to reaction with the lanthanide or uranium reagents, given all of the prior evidence we have of dinitrogen incorporation with this rhenium metalate.[119] Still, the ability to bind these electrophilic Ln^{3+} and U^{3+} ions through the distal diazenido nitrogen in an end-on fashion is unusual. Indeed, there are only two reported systems that display end-on coordination of any N_2 fragment to a lanthanide in the literature,[120,121,124] whether in a mono- or bimetallic fashion. Instead, lanthanide dinitrogen complexes are primarily found as side-on/side-on adducts.[122,123] Similarly, end-on coordination of a dinitrogen fragment to an actinide is rare, with only two reported examples of bimetallic diazenido complexes[133,134] and one example of a monometallic uranium dinitrogen complex.[135] In any case, our surprising results leading to the synthesis of bridging rhenium heterobimetallic diazenido complexes has expanded our understanding of diazenido-type bonding with lanthanide and actinide centers.

Table 1. Select bond distances (Å) and angles (degrees) in **2-Ln** (Ln = Gd, Er), **3-Er**, and **4-U**.

complex	Re–N1	Ln/U–N2	N1–N2	Re1–N1–N2	M1–N2–N1
2-Gd	1.822(5)	2.295(5)	1.191(7)	172.9(4)	177.8(4)
2-Er	1.813(6)	2.179(6)	1.193(8)	170.6(5)	163.3(5)
3-Er[a]	1.831(3), 1.828(2)	2.272(3), 2.264(3)	1.170(4), 1.179(4)	176.8(2), 171.2(2)	171.9(2), 160.8(2)
4-U[a]	1.862(8), 1.873(8)	2.446(9), 2.448(9)	1.17(2), 1.16(2)	174(2), 173.0(7)	157.4(8), 157.6(9)

[a]There are two molecular units within the asymmetric unit.

Ln^{2+} and Homoleptic Inverse Sandwich Complexes

Thus far, we have only discussed reactions with trivalent lanthanide and uranium reagents, and all of the resulting inverse sandwich products, including **1-Ln** and **2-Ln**, have been supported with an L-type, THF ligand. As a means of extending the inverse sandwich binding motif to a wider range of complexes, we also attempted to bind the [(η^5-Cp)Re(BDI)] metalloligand to lanthanides in the 2+ oxidation state, and separately, to isolate an inverse sandwich complex that did not require an additional L-type supporting ligand. We found that reactions between Na[Re(η^5-Cp)(BDI)] and $YbI_2(THF)_2$ successfully led to the isolation of double inverse sandwich complex Yb[(μ-η^5:η^5-Cp)Re(BDI)]$_2$(THF)$_2$ (**5-Yb**, Scheme 5). Despite running this reaction at −78 ºC (which we found necessary to cleanly isolate the products in good yield), we did not observe any evidence suggesting simultaneous formation of any diazenido type minor products. The crystal structure of **5-Yb** was generally consistent with other inverse sandwich complexes **1-Ln** in terms of short Re–Cp distances and Ln–Cp distances trending with ionic radius (Figure 8, Table 2). However, compared with the trivalent inverse sandwich complexes (**1-Ln**), the contraction of the Re–Cp

bond in this divalent structure is on the lower end, with the Re–Cp(cent) distance measuring 1.776(7) Å (Figure 2).

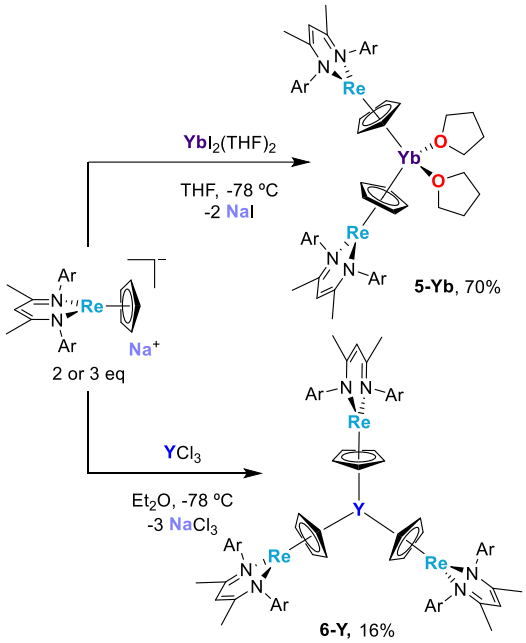

Scheme 5. Syntheses of double inverse sandwich complex **5-Yb** and base-free triple inverse sandwich complex **6-Y**.

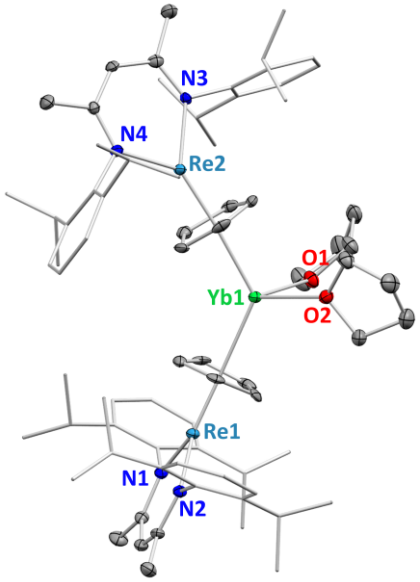

Figure 8. X-ray crystal structure of **5-Yb** shown with 50% probability ellipsoids. The BDI aryl groups are shown in wireframe, and hydrogen atoms are omitted for clarity.

Table 2. Select average (mean) bond distances (Å) in **5-Yb** and **6-Y**.

complex	Re–Cp(cent)	Re–Cp(C)	Ln–Cp(cent)	Ln–Cp(C)	Ln–O	Re–N
5-Yb	1.776	2.159	2.417	2.710	2.416	2.045
6-Y	1.760	2.151	2.339	2.645	–	2.036

As for isolating a base-free inverse sandwich complex in the absence of L-type donors, we speculated that it would be necessary to use either a heavy lanthanide or similar metals with smaller ionic radii and lower preferred coordination numbers. As such, we attempted reactions between Na[Re(η^5-Cp)(BDI)] and several non-solvated heavy lanthanide reagents, as well as other rare earth metals including YCl_3, using Et_2O as the solvent as opposed to THF.[136] Despite observing consumption of the YCl_3 starting material during these reactions, we had difficulty isolating crystalline products, though we were finally able to crystallize a small amount of product Y[(μ-η^5:η^5-Cp)Re(BDI)]$_3$ (**6-Y**) from a toluene/pentane mixture (Scheme 5). An infrared spectrum of crude material included a stretching frequency at 1714 cm^{-1} that could be attributed to possible dinitrogen incorporation, suggesting that a limiting factor in the yield of **6-Y** may be concurrent formation of a diazenido side product. Regardless, the ^{1}H NMR spectra of pure **6-Y** had an absence of THF or other L-type adduct resonances (Figure S18) and the solid-state structure confirmed the synthesis of a homoleptic, base-free triple inverse sandwich complex (Figure 9). The bonding metrics of **6-Y** were also in line with those of other inverse sandwich complexes reported herein (Table 2, Figure 2), with no major deviations from those THF supported species. However, the Re–Cp(cent) distance was on the shorter end at 1.760(6) Å. Given our inability to isolate any early lanthanide or uranium triple inverse sandwich complexes without an L-type adduct, the smaller ionic radius of Y^{3+} is likely the key to formation of the base-free species, though it is less stable and more difficult to isolate in good yield relative to the base-stabilized analogs.

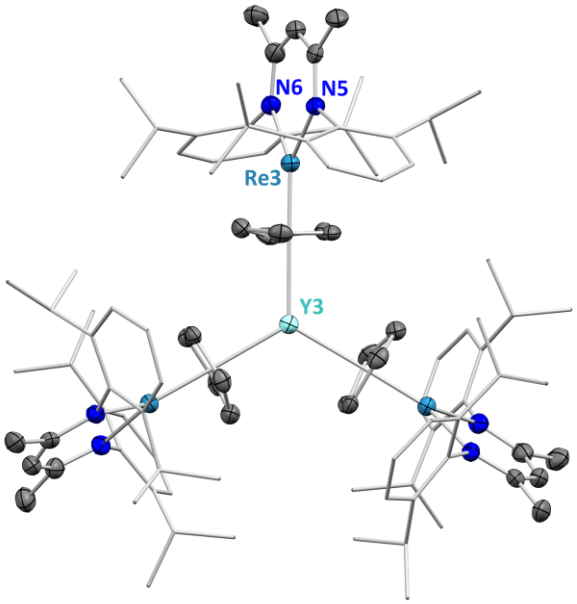

Figure 9. X-ray crystal structure of **6-Y** shown with 50% probability ellipsoids. The BDI aryl groups are shown in wireframe, and hydrogen atoms are omitted for clarity.

Concluding Remarks

We have synthesized a series of tri-rhenium triple inverse sandwich complexes with the early lanthanides, extending the scope of a bonding motif first observed by our group with uranium. These complexes adopt similar bonding metrics to that observed previously with uranium, with the main feature

being shortened Re–Cp bonds due to a decrease in electrostatic repulsions upon bonding to electrophilic lanthanide ions. Moving across the lanthanide series, we observe a break in reactivity at gadolinium, wherein the heavier lanthanides do not adopt a triple inverse sandwich geometry but instead form diazenido-double inverse sandwich type complexes, likely due to their smaller ionic radii and lower preferred coordination numbers. The unexpected formation of end-on lanthanide diazenido complexes led us to pursue the synthesis of similar diazenido species with other lanthanides and uranium. Collectively, these lanthanide- and actinide-rhenium heterobimetallic diazenidos are noteworthy given the scarcity of reported end-on coordination of dinitrogen to *f*-block elements. As such, they represent an expansion in known dinitrogen coordination modes and broaden our understanding of diazenido interactions in the *f*-block. Finally, we were successfully able to expand the inverse sandwich bonding motif with this rhenium metalloligand to both a divalent lanthanide ion as well as to isolate the first base-free, homoleptic triple inverse sandwich complex with this system. Future efforts are underway to study both the reactivity and magnetic properties of these unique compounds, as well as to extend this modular synthetic approach to the synthesis of rhenium inverse sandwich complexes with other metals.

Supporting Information

Experimental procedures, NMR data, FTIR data, crystallographic data, and computational details

Accession Codes

CCDC 2303401–2303412 contain the supplementary crystallographic data for this paper.

Author Information

Notes

The authors declare no competing financial interest. No uncommon safety hazards are noted.

Acknowledgements

This research was funded by the NSF (Grant No. CHE-1465188 and 1954612 to J.A. and R.G.B.). The authors thank the U.S. Department of Energy (DOE) National Nuclear Security Administration through the Nuclear Science and Security Consortium for a fellowship (to I.J.B.) under Award No. DE-NA0003996. The authors thank Dr. Hasan Celik and UC Berkeley's NMR facility in the College of Chemistry (CoC-NMR) for spectroscopic assistance. Instruments in the CoC-NMR are supported in part by NIH S10OD024998. Dr. Simon J. Teat is thanked for his assistance during crystallography experiments at the Advanced Light Source (ALS), and the ALS is supported by the Director, Office of Science, Office of Basic Energy Sciences, of the U.S. DOE under Contract No. DE-AC02-05CH11231. Christopher Ye and David Hales are thanked for helpful discussions and proofreading. Prof. Simon Humphrey (University of Texas, Austin) is thanked for a generous donation of rhenium. L.M. is a senior member of the Institut Universitaire de France. CalMip is acknowledged for a generous grant of computing time.

References

(1) Bochkarev, M. N.; Fedushkin, I. L.; Fagin, A. A.; Petrovskaya, T. V.; Ziller, J. W.; Broomhall-Dillard, R. N. R.; Evans, W. J. Synthesis and Structure of the First Molecular Thulium(II) Complex: [TmI2(MeOCH2CH2OMe)2]. *Angew. Chemie (International Ed. English)* **1997**, *36* (1–2), 133–135. https://doi.org/10.1002/anie.199701331.

(2) Cassani, M. C.; Duncalf, D. J.; Lappert, M. F. The First Example of a Crystalline Subvalent

Organolanthanum Complex: [K([18]Crown-6)- (H2-C6H6)2][(LaCp(Tt)2)2(μ-H6:H6-C6H6)] · 2C6H6 (Cp(Tt) =η5-C5H3Bu(t)2-1,3) [2]. *J. Am. Chem. Soc.* **1998**, *120* (49), 12958–12959. https://doi.org/10.1021/ja980377t.

(3) Bochkarev, M. N. Molecular Compounds of "New" Divalent Lanthanides. *Coord. Chem. Rev.* **2004**, *248* (9–10), 835–851. https://doi.org/10.1016/j.ccr.2004.04.004.

(4) Hitchcock, P. B.; Lappert, M. F.; Maron, L.; Protchenko, A. V. Lanthanum Does Form Stable Molecular Compounds in the +2 Oxidation State. *Angew. Chemie - Int. Ed.* **2008**, *47* (8), 1488–1491. https://doi.org/10.1002/anie.200704887.

(5) MacDonald, M. R.; Ziller, J. W.; Evans, W. J. Synthesis of a Crystalline Molecular Complex of Y2+, [(18-Crown-6)K][(C5H4SiMe3)3Y]. *J. Am. Chem. Soc.* **2011**, *133* (40), 15914–15917. https://doi.org/10.1021/ja207151y.

(6) MacDonald, M. R.; Bates, J. E.; Fieser, M. E.; Ziller, J. W.; Furche, F.; Evans, W. J. Expanding Rare-Earth Oxidation State Chemistry to Molecular Complexes of Holmium(II) and Erbium(II). *J. Am. Chem. Soc.* **2012**, *134* (20), 8420–8423. https://doi.org/10.1021/ja303357w.

(7) Macdonald, M. R.; Bates, J. E.; Ziller, J. W.; Furche, F.; Evans, W. J. Completing the Series of +2 Ions for the Lanthanide Elements: Synthesis of Molecular Complexes of Pr2+, Gd2+, Tb2+, and Lu2+. *J. Am. Chem. Soc.* **2013**, *135* (26), 9857–9868. https://doi.org/10.1021/ja403753j.

(8) Nicholas, H. M.; Mills, D. P. Lanthanides: Divalent Organometallic Chemistry. *Encycl. Inorg. Bioinorg. Chem.* **2017**, 1–10. https://doi.org/10.1002/9781119951438.eibc2453.

(9) Suta, M.; Wickleder, C. Synthesis, Spectroscopic Properties and Applications of Divalent Lanthanides Apart from Eu 2+. *J. Lumin.* **2019**, *210*, 210–238. https://doi.org/10.1016/j.jlumin.2019.02.031.

(10) McClain, K. R.; Gould, C. A.; Marchiori, D. A.; Kwon, H.; Nguyen, T. T.; Rosenkoetter, K. E.; Kuzmina, D.; Tuna, F.; Britt, R. D.; Long, J. R.; Harvey, B. G. Divalent Lanthanide Metallocene Complexes with a Linear Coordination Geometry and Pronounced 6s-5d Orbital Mixing. *J. Am. Chem. Soc.* **2022**, *144* (48), 22193–22201. https://doi.org/10.1021/jacs.2c09880.

(11) Gregson, M.; Lu, E.; Mills, D. P.; Tuna, F.; McInnes, E. J. L.; Hennig, C.; Scheinost, A. C.; McMaster, J.; Lewis, W.; Blake, A. J.; Kerridge, A.; Liddle, S. T. The Inverse-Trans-Influence in Tetravalent Lanthanide and Actinide Bis(Carbene) Complexes. *Nat. Commun.* **2017**, *8* (1), 1–11. https://doi.org/10.1038/ncomms14137.

(12) Rice, N. T.; Popov, I. A.; Russo, D. R.; Bacsa, J.; Batista, E. R.; Yang, P.; Telser, J.; La Pierre, H. S. Design, Isolation, and Spectroscopic Analysis of a Tetravalent Terbium Complex. *J. Am. Chem. Soc.* **2019**, *141* (33), 13222–13233. https://doi.org/10.1021/jacs.9b06622.

(13) Xue, T.; Ding, Y.-S.; Jiang, X.-L.; Tao, L.; Li, J.; Zheng, Z. Tetravalent Terbium Chelates: Stability Enhancement and Property Tuning. *Precis. Chem.* **2023**, *1* (10), 583–591. https://doi.org/10.1021/prechem.3c00065.

(14) Palumbo, C. T.; Zivkovic, I.; Scopelliti, R.; Mazzanti, M. Molecular Complex of Tb in the +4 Oxidation State. *J. Am. Chem. Soc.* **2019**, *141* (25), 9827–9831. https://doi.org/10.1021/jacs.9b05337.

(15) Li, N.; Zhang, W. X. Molecular Complexes of Emerging Tetravalent Rare-Earth Metals. *Chinese J. Chem.* **2020**, *38* (11), 1449–1450. https://doi.org/10.1002/cjoc.202000258.

(16) Willauer, A. R.; Palumbo, C. T.; Fadaei-Tirani, F.; Zivkovic, I.; Douair, I.; Maron, L.; Mazzanti,

M. Accessing the +IV Oxidation State in Molecular Complexes of Praseodymium. *J. Am. Chem. Soc.* **2020**, *142* (12), 5538–5542. https://doi.org/10.1021/jacs.0c01204.

(17) Willauer, A. R.; Palumbo, C. T.; Scopelliti, R.; Zivkovic, I.; Douair, I.; Maron, L.; Mazzanti, M. Stabilization of the Oxidation State +IV in Siloxide-Supported Terbium Compounds. *Angew. Chemie - Int. Ed.* **2020**, *59* (9), 3549–3553. https://doi.org/10.1002/anie.201914733.

(18) Rice, N. T.; Popov, I. A.; Russo, D. R.; Gompa, T. P.; Ramanathan, A.; Bacsa, J.; Batista, E. R.; Yang, P.; La Pierre, H. S. Comparison of Tetravalent Cerium and Terbium Ions in a Conserved, Homoleptic Imidophosphorane Ligand Field. *Chem. Sci.* **2020**, *11* (24), 6149–6159. https://doi.org/10.1039/d0sc01414a.

(19) Gompa, T. P.; Ramanathan, A.; Rice, N. T.; La Pierre, H. S. The Chemical and Physical Properties of Tetravalent Lanthanides: Pr, Nd, Tb, and Dy. *Dalt. Trans.* **2020**, *49* (45), 15945–15987. https://doi.org/10.1039/d0dt01400a.

(20) Willauer, A. R.; Douair, I.; Chauvin, A. S.; Fadaei-Tirani, F.; Bünzli, J. C. G.; Maron, L.; Mazzanti, M. Structure, Reactivity and Luminescence Studies of Triphenylsiloxide Complexes of Tetravalent Lanthanides. *Chem. Sci.* **2022**, *13* (3), 681–691. https://doi.org/10.1039/d1sc05517h.

(21) Shafi, Z.; Gibson, J. K. Lanthanide Complexes Containing a Terminal Ln=O Oxo Bond: Revealing Higher Stability of Tetravalent Praseodymium versus Terbium. *Inorg. Chem.* **2022**. https://doi.org/10.1021/acs.inorgchem.2c00525.

(22) Chilton, N. F.; Collison, D.; McInnes, E. J. L.; Winpenny, R. E. P.; Soncini, A. An Electrostatic Model for the Determination of Magnetic Anisotropy in Dysprosium Complexes. *Nat. Commun.* **2013**, *4* (1), 1–7. https://doi.org/10.1038/ncomms3551.

(23) Woodruff, D. N.; Winpenny, R. E. P.; Layfield, R. A. Lanthanide Single-Molecule Magnets. *Chem. Rev.* **2013**, *113* (7), 5110–5148. https://doi.org/10.1021/CR400018Q/ASSET/IMAGES/LARGE/CR-2013-00018Q_0038.JPEG.

(24) Zhu, Z.; Tang, J. Lanthanide Single-Molecule Magnets with High Anisotropy Barrier: Where to from Here? *Natl. Sci. Rev.* **2022**, *9* (12). https://doi.org/10.1093/nsr/nwac194.

(25) Gould, C. A.; McClain, K. R.; Reta, D.; Kragskow, J. G. C.; Marchiori, D. A.; Lachman, E.; Choi, E. S.; Analytis, J. G.; Britt, R. D.; Chilton, N. F.; Harvey, B. G.; Long, J. R. Ultrahard Magnetism from Mixed-Valence Dilanthanide Complexes with Metal-Metal Bonding. *Science (80-.).* **2022**, *375* (6577), 198–202. https://doi.org/10.1126/science.abl5470.

(26) Meihaus, K. R.; Fieser, M. E.; Corbey, J. F.; Evans, W. J.; Long, J. R. Record High Single-Ion Magnetic Moments Through 4fn5d1 Electron Configurations in the Divalent Lanthanide Complexes [(C5H4SiMe3)3Ln]-. *J. Am. Chem. Soc.* **2015**, *137* (31), 9855–9860. https://doi.org/10.1021/jacs.5b03710.

(27) Gregson, M.; Chilton, N. F.; Ariciu, A. M.; Tuna, F.; Crowe, I. F.; Lewis, W.; Blake, A. J.; Collison, D.; McInnes, E. J. L.; Winpenny, R. E. P.; Liddle, S. T. A Monometallic Lanthanide Bis(Methanediide) Single Molecule Magnet with a Large Energy Barrier and Complex Spin Relaxation Behaviour. *Chem. Sci.* **2016**, *7* (1), 155–165. https://doi.org/10.1039/c5sc03111g.

(28) Ding, Y. S.; Chilton, N. F.; Winpenny, R. E. P.; Zheng, Y. Z. On Approaching the Limit of Molecular Magnetic Anisotropy: A Near-Perfect Pentagonal Bipyramidal Dysprosium(III) Single-Molecule Magnet. *Angew. Chemie - Int. Ed.* **2016**, *55* (52), 16071–16074. https://doi.org/10.1002/anie.201609685.

(29) Goodwin, C. A. P.; Ortu, F.; Reta, D.; Chilton, N. F.; Mills, D. P. Molecular Magnetic Hysteresis

at 60 Kelvin in Dysprosocenium. *Nature* **2017**, *548* (7668), 439–442. https://doi.org/10.1038/nature23447.

(30) Demir, S.; Gonzalez, M. I.; Darago, L. E.; Evans, W. J.; Long, J. R. Giant Coercivity and High Magnetic Blocking Temperatures for N23- Radical-Bridged Dilanthanide Complexes upon Ligand Dissociation /639/638/263/406 /639/638/911 /639/638/298/920 Article. *Nat. Commun.* **2017**, *8* (1), 1–9. https://doi.org/10.1038/s41467-017-01553-w.

(31) Dey, A.; Kalita, P.; Chandrasekhar, V. Lanthanide(III)-Based Single-Ion Magnets. *ACS Omega* **2018**, *3* (8), 9462–9475. https://doi.org/10.1021/ACSOMEGA.8B01204/ASSET/IMAGES/LARGE/AO-2018-012044_0013.JPEG.

(32) Evans, P.; Reta, D.; Whitehead, G. F. S.; Chilton, N. F.; Mills, D. P. Bis-Monophospholyl Dysprosium Cation Showing Magnetic Hysteresis at 48 K. *J. Am. Chem. Soc.* **2019**, *141* (50), 19935–19940. https://doi.org/10.1021/jacs.9b11515.

(33) Thomas-Hargreaves, L. R.; Giansiracusa, M. J.; Gregson, M.; Zanda, E.; O'Donnell, F.; Wooles, A. J.; Chilton, N. F.; Liddle, S. T. Correlating Axial and Equatorial Ligand Field Effects to the Single-Molecule Magnet Performances of a Family of Dysprosium Bis-Methanediide Complexes. *Chem. Sci.* **2021**, *12* (11), 3911–3920. https://doi.org/10.1039/d1sc00238d.

(34) Bünzli, J.-C. G.; Eliseeva, S. V. Basics of Lanthanide Photophysics; Springer, Berlin, Heidelberg, 2010; pp 1–45. https://doi.org/10.1007/4243_2010_3.

(35) Bünzli, J. C. G. Lanthanide Luminescence for Biomedical Analyses and Imaging. *Chem. Rev.* **2010**, *110* (5), 2729–2755. https://doi.org/10.1021/cr900362e.

(36) Bünzli, J. C. G. Lanthanide Luminescence: From a Mystery to Rationalization, Understanding, and Applications. *Handb. Phys. Chem. Rare Earths* **2016**, *50*, 141–176. https://doi.org/10.1016/bs.hpcre.2016.08.003.

(37) Hasegawa, M.; Ohmagari, H.; Tanaka, H.; Machida, K. Luminescence of Lanthanide Complexes: From Fundamental to Prospective Approaches Related to Water- and Molecular-Stimuli. *J. Photochem. Photobiol. C Photochem. Rev.* **2022**, *50*, 100484. https://doi.org/10.1016/j.jphotochemrev.2022.100484.

(38) Vaidyanathan, S. Recent Progress on Lanthanide-Based Long Persistent Phosphors: An Overview. *J. Mater. Chem. C* **2023**. https://doi.org/10.1039/D2TC05243A.

(39) Evans, W. J.; Champagne, T. M.; Ziller, J. W. Samarium versus Aluminium Lewis Acidity in a Mixed Alkyl Carboxylate Complex Related to Alkylaluminium Activation in Diene Polymerization Catalysis. *Chem. Commun.* **2005**, No. 47, 5925–5927. https://doi.org/10.1039/b511714c.

(40) Qiao, Y.; Schelter, E. J. Lanthanide Photocatalysis. *Acc. Chem. Res.* **2018**, *51* (11), 2926–2936. https://doi.org/10.1021/acs.accounts.8b00336.

(41) Jenks, T. C.; Bailey, M. D.; Hovey, J. L.; Fernando, S.; Basnayake, G.; Cross, M. E.; Li, W.; Allen, M. J. First Use of a Divalent Lanthanide for Visible-Light-Promoted Photoredox Catalysis. *Chem. Sci.* **2018**, *9* (5), 1273–1278. https://doi.org/10.1039/c7sc02479g.

(42) Tamang, S. R.; Singh, A.; Bedi, D.; Bazkiaei, A. R.; Warner, A. A.; Glogau, K.; McDonald, C.; Unruh, D. K.; Findlater, M. Polynuclear Lanthanide–Diketonato Clusters for the Catalytic Hydroboration of Carboxamides and Esters. *Nat. Catal.* **2020**, *3* (2), 154–162. https://doi.org/10.1038/s41929-019-0405-5.

(43) Hou, W.; Wang, G.; Wu, X.; Sun, S.; Zhao, C.; Liu, W. S.; Pan, F. Lanthanide Clusters as Highly Efficient Catalysts Regarding Carbon Dioxide Activation. *New J. Chem.* **2020**, *44* (13), 5019–5022. https://doi.org/10.1039/c9nj05831a.

(44) Dicken, R. D.; Motta, A.; Marks, T. J. Homoleptic Lanthanide Amide Catalysts for Organic Synthesis: Experiment and Theory. *ACS Catal.* **2021**, *11* (5), 2715–2734. https://doi.org/10.1021/acscatal.0c04882.

(45) Rothbaum, J. O.; Motta, A.; Kratish, Y.; Marks, T. J. Chemodivergent Organolanthanide-Catalyzed C-H α-Mono-Borylation of Pyridines. *J. Am. Chem. Soc.* **2022**, *144* (37), 17086–17096. https://doi.org/10.1021/jacs.2c06844.

(46) Kynman, A. E.; Elghanayan, L. K.; Desnoyer, A. N.; Yang, Y.; Sévery, L.; Di Giuseppe, A.; Tilley, T. D.; Maron, L.; Arnold, P. L. Controlled Monodefluorination and Alkylation of C(Sp3)-F Bonds by Lanthanide Photocatalysts: Importance of Metal-Ligand Cooperativity. *Chem. Sci.* **2022**, *13* (47), 14090–14100. https://doi.org/10.1039/d2sc04192h.

(47) Lam, F. Y. T.; Wong, A.; Trinh, T. M.; Kelly, R. P.; Rao, G.; David Britt, R.; Arnold, P. L. Ln N2RR 1 Catalytic Dinitrogen Reduction by Earth-Abundant Lanthanide Complexes. **2022**. https://doi.org/10.26434/CHEMRXIV-2022-GX6XL.

(48) Persson, I.; D'Angelo, P.; De Panfilis, S.; Sandström, M.; Eriksson, L. Hydration of Lanthanoid(III) Ions in Aqueous Solution and Crystalline Hydrates Studied by EXAFS Spectroscopy and Crystallography: The Myth of the "Gadolinium Break." *Chem. - A Eur. J.* **2008**, *14* (10), 3056–3066. https://doi.org/10.1002/chem.200701281.

(49) Laing, M. Gadolinium: Central Metal of the Lanthanoids. *J. Chem. Educ.* **2009**, *86* (2), 188–189. https://doi.org/10.1021/ed086p188.

(50) Eulgem, P. J.; Klein, A.; Maggiarosa, N.; Naumann, D.; Pohl, R. W. H. New Rare Earth Metal Complexes with Nitrogen-Rich Ligands: 5,5′-Bitetrazolate and 1,3-Bis(Tetrazol-5-Yl)Triazenate - On the Borderline between Coordination and the Formation of Salt-like Compounds. *Chem. - A Eur. J.* **2008**, *14* (12), 3727–3736. https://doi.org/10.1002/chem.200702006.

(51) Steinhauser, G.; Giester, G.; Leopold, N.; Wagner, C.; Villa, M.; Musilek, A. Nitrogen-Rich Compounds of the Lanthanoids: Highlights and Summary. *Helv. Chim. Acta* **2010**, *93* (2), 183–202. https://doi.org/10.1002/hlca.200900389.

(52) Knoll, C.; Müller, D.; Giester, G.; Ofner, J.; Lendl, B.; Weinberger, P.; Steinhauser, G. An Unusually Water-Poor 5,5′-Azobistetrazolate of Dysprosium: Stabilization of a Nitrogen-Rich Heterocycle by a Minimum of Hydrogen Bonds. *New J. Chem.* **2013**, *37* (12), 3840–3844. https://doi.org/10.1039/c3nj00492a.

(53) Cable, M. L.; Kirby, J. P.; Gray, H. B.; Ponce, A. Enhancement of Anion Binding in Lanthanide Optical Sensors. *Acc. Chem. Res.* **2013**, *46* (11), 2576–2584. https://doi.org/10.1021/ar400050t.

(54) Babailov, S. P.; Chuikov, I. P.; Kruppa, A. I. Activation Energies of Intermolecular Dynamics in Ethylenediaminetetraacetate Complexes with Lanthanides: An Effect of the "Gadolinium Break." *Inorganica Chim. Acta* **2016**, *439*, 117–122. https://doi.org/10.1016/j.ica.2015.10.009.

(55) Demakov, P. A.; Sapchenko, S. A.; Samsonenko, D. G.; Dybtsev, D. N.; Fedin, V. P. Gadolinium Break in a Series of Three-Dimensional Trans-1,4-Cyclohexane Dicarboxylates of Rare Earth Elements. *J. Struct. Chem.* **2019**, *60* (5), 815–822. https://doi.org/10.1134/S0022476619050159.

(56) Welch, J. M.; Müller, D.; Knoll, C.; Wilkovitsch, M.; Giester, G.; Ofner, J.; Lendl, B.; Weinberger, P.; Steinhauser, G. Picomolar Traces of Americium(III) Introduce Drastic Changes in

the Structural Chemistry of Terbium(III): A Break in the "Gadolinium Break." *Angew. Chemie - Int. Ed.* **2017**, *56* (43), 13264–13269. https://doi.org/10.1002/anie.201703971.

(57) Müller, D.; Knoll, C.; Herrmann, A.; Savasci, G.; Welch, J. M.; Artner, W.; Ofner, J.; Lendl, B.; Giester, G.; Weinberger, P.; Steinhauser, G. Azobis[Tetrazolide]-Carbonates of the Lanthanides – Breaking the Gadolinium Break. *Eur. J. Inorg. Chem.* **2018**, *2018* (19), 1969–1975. https://doi.org/10.1002/ejic.201800218.

(58) Aguilà, D.; Barrios, L. A.; Velasco, V.; Roubeau, O.; Repollés, A.; Alonso, P. J.; Sesé, J.; Teat, S. J.; Luis, F.; Aromí, G. Heterodimetallic [LnLn'] Lanthanide Complexes: Toward a Chemical Design of Two-Qubit Molecular Spin Quantum Gates. *J. Am. Chem. Soc.* **2014**, *136* (40), 14215–14222. https://doi.org/10.1021/ja507809w.

(59) Burns, C. P.; Yang, X.; Sung, S.; Wofford, J. D.; Bhuvanesh, N. S.; Hall, M. B.; Nippe, M. Towards Understanding of Lanthanide-Transition Metal Bonding: Investigations of the First Ce-Fe Bonded Complex. *Chem. Commun.* **2018**, *54* (77), 10893–10896. https://doi.org/10.1039/c8cc05243c.

(60) Burns, C. P.; Yang, X.; Wofford, J. D.; Bhuvanesh, N. S.; Hall, M. B.; Nippe, M. Structure and Magnetization Dynamics of Dy−Fe and Dy−Ru Bonded Complexes. *Angew. Chemie - Int. Ed.* **2018**, *57* (27), 8144–8148. https://doi.org/10.1002/anie.201803761.

(61) Sørensen, T. J.; Faulkner, S. Multimetallic Lanthanide Complexes: Using Kinetic Control to Define Complex Multimetallic Arrays. *Acc. Chem. Res.* **2018**, *51* (10), 2493–2501. https://doi.org/10.1021/acs.accounts.8b00205.

(62) Yang, X.; Burns, C. P.; Nippe, M.; Hall, M. B. Unsupported Lanthanide-Transition Metal Bonds: Ionic vs Polar Covalent? *Inorg. Chem.* **2021**, *60* (13), 9394–9401. https://doi.org/10.1021/acs.inorgchem.1c00285.

(63) Swain, A.; Sen, A.; Rajaraman, G. Are Lanthanide-Transition Metal Direct Bonds a Route to Achieving New Generation {3d-4f} SMMs? *Dalt. Trans.* **2021**, *50* (44), 16099–16109. https://doi.org/10.1039/d1dt02256c.

(64) Krisyuk, V. V.; Urkasym Kyzy, S.; Rybalova, T. V.; Korolkov, I. V.; Grebenkina, M. A.; Lavrov, A. N. Structure and Properties of Heterometallics Based on Lanthanides and Transition Metals with Methoxy-β-Diketonates. *Molecules* **2022**, *27* (23), 8400. https://doi.org/10.3390/molecules27238400.

(65) Boreen, M. A.; Lohrey, T. D.; Rao, G.; Britt, R. D.; Maron, L.; Arnold, J.; David Britt, R.; Maron, L.; Arnold, J. A Uranium Tri-Rhenium Triple Inverse Sandwich Compound. *J. Am. Chem. Soc.* **2019**, *141* (13), 5144–5148. https://doi.org/10.1021/jacs.9b01331.

(66) Schumann, H.; Winterfeld, J.; Esser, L.; Kociok-Köhn, G. [{(Me3Si)2N}2Sm{μ(H8:H8-C8H8)}-Sm{N(SiMe3)2}2]: An Inverse Organolanthanoid Sandwich Complex. *Angew. Chemie Int. Ed. English* **1993**, *32* (8), 1208–1210. https://doi.org/10.1002/anie.199312081.

(67) Evans, W. J.; Johnston, M. A.; Clark, R. D.; Anwander, R.; Ziller, J. W. Heteroleptic and Heterometallic Divalent Lanthanide Bis(Trimethylsilyl)Amide Complexes: Mixed Ligand, Inverse Sandwich, and Alkali Metal Derivatives. *Polyhedron* **2001**, *20* (19), 2483–2490. https://doi.org/10.1016/S0277-5387(01)00848-8.

(68) Nishiura, M.; Hou, Z.; Wakatsuki, Y. A Novel Binuclear Samarium(II) Complex Bearing Mixed Cyclopentadienide/Siloxide Ligands: [(C5Me 5)Sm-{μ-OSi(OtBu)3}3Sm]. Synthesis, Structure, Electron-Transfer, and Unusual Metal-Coordination Reactions. *Organometallics* **2004**, *23* (6),

1359–1368. https://doi.org/10.1021/om0343418.

(69) Edelmann, A.; Blaurock, S.; Lorenz, V.; Hilfert, L.; Edelmann, F. T. [(C5Me5)Yb(μ-H8,H8-Cot‴)Yb(μ-H8,H8-Cot‴)Yb(C 5Me5)] - A Unique Tetradecker Sandwich Complex of a Divalent Lanthanide. *Angew. Chemie - Int. Ed.* **2007**, *46* (35), 6732–6734. https://doi.org/10.1002/anie.200702148.

(70) Lorenz, V.; Edelmann, A.; Blaurock, S.; Freise, F.; Edelmann, F. T. A Unique Organolanthanide Cluster Containing Bulky Cyclooctatetraenyl Ligands. *Organometallics* **2007**, *26* (19), 4708–4710. https://doi.org/10.1021/om700589r.

(71) Summerscales, O. T.; Jones, S. C.; Geoffrey N Cloke, F.; Hitchcock, P. B. Anti-Bimetallic Complexes of Divalent Lanthanides with Silylated Pentalene and Cyclooctatetraenyl Bridging Ligands as Molecular Models for Lanthanide-Based Polymers. *Organometallics* **2009**, *28* (20), 5896–5908. https://doi.org/10.1021/om900520h.

(72) Lorenz, V.; Blaurock, S.; Hrib, C. G.; Edelmann, F. T. The First Linear, Homoleptic Triple-Decker Sandwich Complex of an f-Element: A Molecular Model for Organolanthanide Nanowires. *Organometallics* **2010**, *29* (21), 4787–4789. https://doi.org/10.1021/om1004385.

(73) Lorenz, V.; Blaurock, S.; Hrib, C. G.; Edelmann, F. T. Encapsulation of Cyclooctatetraenyl Dianion in an Unusual Organic/Inorganic Lanthanide Triple-Decker Sandwich Complex. *Dalt. Trans.* **2010**, *39* (29), 6629–6631. https://doi.org/10.1039/c0dt00094a.

(74) Le Roy, J. J.; Jeletic, M.; Gorelsky, S. I.; Korobkov, I.; Ungur, L.; Chibotaru, L. F.; Murugesu, M. An Organometallic Building Block Approach to Produce a Multidecker 4 f Single-Molecule Magnet. *J. Am. Chem. Soc.* **2013**, *135* (9), 3502–3510. https://doi.org/10.1021/ja310642h.

(75) Edelmann, A.; Lorenz, V.; Hrib, C. G.; Hilfert, L.; Blaurock, S.; Edelmann, F. T. Steric Effects in Lanthanide Sandwich Complexes Containing Bulky Cyclooctatetraenyl Ligands. *Organometallics* **2013**, *32* (5), 1435–1444. https://doi.org/10.1021/om3010993.

(76) Huang, W.; Dulong, F.; Wu, T.; Khan, S. I.; Miller, J. T.; Cantat, T.; Diaconescu, P. L. A Six-Carbon 10π-Electron Aromatic System Supported by Group 3 Metals. *Nat. Commun.* **2013**, *4* (1), 1–7. https://doi.org/10.1038/ncomms2473.

(77) Evans, W. J.; Shreeve, J. L.; Ziller, J. W. Synthesis and Structure of Inverse Cyclooctatetraenyl Sandwich Complexes of Europium(II): [(C5Me5)(THF)2Eu]2(μ-C8H8 and [(THF)3K(μ-C8H8)]2Eu. *Polyhedron* **1995**, *14* (20–21), 2945–2951. https://doi.org/10.1016/0277-5387(95)00162-L.

(78) Le Roy, J. J.; Ungur, L.; Korobkov, I.; Chibotaru, L. F.; Murugesu, M. Coupling Strategies to Enhance Single-Molecule Magnet Properties of Erbium-Cyclooctatetraenyl Complexes. *J. Am. Chem. Soc.* **2014**, *136* (22), 8003–8010. https://doi.org/10.1021/ja5022552.

(79) Kotyk, C. M.; Fieser, M. E.; Palumbo, C. T.; Ziller, J. W.; Darago, L. E.; Long, J. R.; Furche, F.; Evans, W. J. Isolation of +2 Rare Earth Metal Ions with Three Anionic Carbocyclic Rings: Bimetallic Bis(Cyclopentadienyl) Reduced Arene Complexes of La2+ and Ce2+ Are Four Electron Reductants. *Chem. Sci.* **2015**, *6* (12), 7267–7273. https://doi.org/10.1039/c5sc02486b.

(80) Huang, W.; Le Roy, J. J.; Khan, S. I.; Ungur, L.; Murugesu, M.; Diaconescu, P. L. Tetraanionic Biphenyl Lanthanide Complexes as Single-Molecule Magnets. *Inorg. Chem.* **2015**, *54* (5), 2374–2382. https://doi.org/10.1021/ic5029788.

(81) Sroor, F. M.; Hrib, C. G.; Liebing, P.; Hilfert, L.; Busse, S.; Edelmann, F. T. Five Different Types of H8-Cyclooctatetraenyl-Lanthanide Half-Sandwich Complexes from One Ligand Set, Including

a “Giant Neodymium Wheel.” *Dalt. Trans.* **2016**, *45* (34), 13332–13346. https://doi.org/10.1039/c6dt01974a.

(82) Selikhov, A. N.; Mahrova, T. V.; Cherkasov, A. V.; Fukin, G. K.; Kirillov, E.; Alvarez Lamsfus, C.; Maron, L.; Trifonov, A. A. Yb(II) Triple-Decker Complex with the μ-Bridging Naphthalene Dianion [CpBn5Yb(DME)]2(μ-H4:H4-C10H8). Oxidative Substitution of [C10H8]2- by 1,4-Diphenylbuta-1,3-Diene and P4 and Protonolysis of the Yb-C10H8 Bond by PhPH2. *Organometallics* **2016**, *35* (14), 2401–2409. https://doi.org/10.1021/acs.organomet.6b00428.

(83) Harriman, K. L. M.; Le Roy, J. J.; Ungur, L.; Holmberg, R. J.; Korobkov, I.; Murugesu, M. Cycloheptatrienyl Trianion: An Elusive Bridge in the Search of Exchange Coupled Dinuclear Organolanthanide Single-Molecule Magnets. *Chem. Sci.* **2016**, *8* (1), 231–240. https://doi.org/10.1039/C6SC01224H.

(84) Kelly, R. P.; Maron, L.; Scopelliti, R.; Mazzanti, M. Reduction of a Cerium(III) Siloxide Complex To Afford a Quadruple-Decker Arene-Bridged Cerium(II) Sandwich. *Angew. Chemie - Int. Ed.* **2017**, *56* (49), 15663–15666. https://doi.org/10.1002/anie.201709769.

(85) Lorenz, V.; Liebing, P.; Bathelier, A.; Engelhardt, F.; Maron, L.; Hilfert, L.; Busse, S.; Edelmann, F. T. The “Wanderlust” of Me3Si Groups in Rare-Earth Triple-Decker Complexes: A Combined Experimental and Computational Study. *Chem. Commun.* **2018**, *54* (73), 10280–10283. https://doi.org/10.1039/c8cc05317k.

(86) Kelly, R. P.; Toniolo, D.; Tirani, F. F.; Maron, L.; Mazzanti, M. A Tetranuclear Samarium(Ii) Inverse Sandwich from Direct Reduction of Toluene by a Samarium(Ii) Siloxide. *Chem. Commun.* **2018**, *54* (73), 10268–10271. https://doi.org/10.1039/c8cc04169e.

(87) Greenough, J.; Zhou, Z.; Wei, Z.; Petrukhina, M. A. Versatility of Cyclooctatetraenyl Ligands in Rare Earth Metal Complexes of the [M2(COT)3(THF)2] (M = y and La) Type. *Dalt. Trans.* **2019**, *48* (17), 5614–5620. https://doi.org/10.1039/c9dt00868c.

(88) Apostolidis, C.; Deacon, G. B.; Dornberger, E.; Edelmann, F. T.; Kanellakopulos, B.; MacKinnon, P.; Stalke, D. Crystallization and X-Ray Structures of [NaYb(C5H5)3] and Yb(C5H5)2. *Chem. Commun.* **1997**, No. 11, 1047–1048. https://doi.org/10.1039/a700531h.

(89) Buschmann, D. A.; Dietrich, H. M.; Schneider, D.; Birkelbach, V. M.; Stuhl, C.; Törnroos, K. W.; Maichle-Mössmer, C.; Anwander, R. Nanoscale Organolanthanum Clusters: Nuclearity-Directing Role of Cyclopentadienyl and Halogenido Ligands. *Chem. - A Eur. J.* **2020**, *26* (47), 10834–10840. https://doi.org/10.1002/chem.202001482.

(90) Peedika Paramban, R.; Guo, Z.; Deacon, G. B.; Junk, P. C. Formation of a Cyclooctatetraenylsamarium(Iii) Inverse Sandwich That Ring-Opens Tetrahydrofuran. *Dalt. Trans.* **2023**, *52* (12), 3563–3566. https://doi.org/10.1039/d2dt04164b.

(91) Arliguie, T.; Lance, M.; Nierlich, M.; Ephritikhine, M. Inverse Cycloheptatrienyl Sandwich Complexes of Uranium and Neodymium. *J. Chem. Soc. - Dalt. Trans.* **1997**, No. 14, 2501–2504. https://doi.org/10.1039/a701352c.

(92) Evans, W. J.; Clark, R. D.; Ansari, M. A.; Ziller, J. W. Bent vs Linear Metallocenes Involving C5Me5 vs C8H8 Ligands: Synthesis, Structure, and Reactivity of the Triple-Decked (C5Me5)(THF)(χ)Sm(C8H8)Sm(THF)(χ)(C5Me5) (χ = 0, 1) Complexes Including a Formal Two-Electron Oxidative Addition to a Single Lanthanide . *J. Am. Chem. Soc.* **1998**, *120* (37), 9555–9563. https://doi.org/10.1021/ja980735s.

(93) Evans, W. J.; Greci, M. A.; Johnston, M. A.; Ziller, J. W. Synthesis, Structure, and Reactivity of

Organometallic Lanthanide - Dizirconium Nonaisopropoxide Complexes. *Chem. - A Eur. J.* **1999**, *5* (12), 3482–3486. https://doi.org/10.1002/(sici)1521-3765(19991203)5:12<3482::aid-chem3482>3.3.co;2-p.

(94) Evans, W. J.; Johnston, M. A.; Greci, M. A.; Ziller, J. W. Synthesis, Structure, and Reactivity of Unsolvated Triple-Decked Bent Metallocenes of Divalent Europium and Ytterbium. *Organometallics* **1999**, *18* (8), 1460–1464. https://doi.org/10.1021/om980762r.

(95) Evans, W. J.; Johnston, M. A.; Clark, R. D.; Ziller, J. W. Variability of (Ring Centroid)-Ln-(Ring Ccntroid) Angles in the Mixed Ligand C5Me5/C8H8 Complexes (C5Me5)Ln(C8H8) and [(C5Me5)Yb(THF)](μ-H8 : H8-C8H8)[Yb(C5Me5)]. *J. Chem. Soc. Dalt. Trans.* **2000**, No. 10, 1609–1612. https://doi.org/10.1039/a908412f.

(96) Gun'ko, Y. K.; Hitchcock, P. B.; Lappert, M. F. Nonclassical Organolanthanoid Metal Chemistry: [K([18]-Crown-6)(H2-PhMe)2]X (X = [(LnCpt3)2(μ-H)], [(LnCp″2)2(μ-H6:H6-PhMe)]) from [LnCpx3], K, and [18]-Crown-6 in Toluene (Ln = La, Ce; Cpt =. *Organometallics* **2000**, *19* (15), 2832–2834. https://doi.org/10.1021/om0001873.

(97) Fedushkin, I. L.; Nevodchikov, V. K.; Cherkasov, V. K.; Bochkarev, M. N.; Schumann, H.; Girgsdies, F.; Görlitz, F. H.; Kociok-Köhn, G.; Pickardt, J. Synthesis and Characterization of Eu(II) and Sm(II) Complexes Containing the Cyclopentadienylvanadiumnaphthalene Anion. Molecular Structure of [(C5H5) V(C10H8)]2Eu(THF)(DME) and [(C5H5) V(C10H8) Eu(C5H5)(THF)] η. *J. Organomet. Chem.* **1996**, *511* (1–2), 157–162. https://doi.org/10.1016/0022-328X(95)05923-D.

(98) Grindell, R.; Day, B. M.; Guo, F. S.; Pugh, T.; Layfield, R. A. Activation of C-H Bonds by Rare-Earth Metallocene-Butyl Complexes. *Chem. Commun.* **2017**, *53* (72), 9990–9993. https://doi.org/10.1039/c7cc05597h.

(99) Reactions involving the highly reactive Na[(η^5-Cp)Re(BDI)] metalate often form unwanted side products Re(η^5-Cp)(BDI) and Re(H)(η^5-Cp)(BDI) in the presence of even trace impurities in the starting materials or solvents.

(100) Boreen, M. A.; Arnold, J. Multiple Bonding in Actinide Chemistry. In *Encyclopedia of Inorganic and Bioinorganic Chemistry*; John Wiley & Sons, Ltd, 2018; pp 1–18. https://doi.org/10.1002/9781119951438.eibc2535.

(101) Rogers, R. D.; Atwood, J. L.; Emad, A.; Sikora, D. J.; Rausch, M. D. The Formation and Molecular Structures of (H5-C5H5)3Y · OC4H8 and (H5-C5H5)3La · OC4H8. *J. Organomet. Chem.* **1981**, *216* (3), 383–392. https://doi.org/10.1016/S0022-328X(00)85819-2.

(102) Wenqi, C.; Guanyang, L.; Jusong, X.; Gecheng, W.; Yin, Z.; Zhongsheng, J. Syntheses and Crystal Structures of (H5-C5H5)3Ln(THF) (Ln = Ce, Er). *J. Organomet. Chem.* **1994**, *467* (1), 75–78. https://doi.org/10.1016/0022-328X(94)88010-7.

(103) Junk, P. C. Tris(H5-Cyclopentadienyl)-Tetrahydrofuranpraseodymium. *Appl. Organomet. Chem.* **2003**, *17* (11), 875–876. https://doi.org/10.1002/aoc.549.

(104) Benetollo, F.; Bombieri, G.; Castellani, C. B.; Jahn, W.; Fischer, R. D. The Formation and the Structure of (H5-C5H5)3Nd·OC4H8. *Inorganica Chim. Acta* **1984**, *95* (6), L7–L10. https://doi.org/10.1016/S0020-1693(00)84897-5.

(105) Wang, S.; Yu, Y.; Ye, Z.; Qian, C.; Huang, X. The Formation and Molecular Structure of (H5-C5H5)3Sm · OC4H8. *J. Organomet. Chem.* **1994**, *464* (1), 55–58. https://doi.org/10.1016/0022-328X(94)87008-X.

(106) Rogers, R. D.; Vann Bynum, R.; Atwood, J. L. Synthesis and Structure of (H5-C5H5)3Gd · OC4H8. *J. Organomet. Chem.* **1980**, *192* (1), 65–73. https://doi.org/10.1016/S0022-328X(00)93331-X.

(107) Lohrey, T. D.; Maron, L.; Bergman, R. G.; Arnold, J. Heterotetrametallic Re-Zn-Zn-Re Complex Generated by an Anionic Rhenium(I) β-Diketiminate. *J. Am. Chem. Soc.* **2019**, *141* (2), 800–804. https://doi.org/10.1021/jacs.8b12494.

(108) Becke, A. D. Density-Functional Thermochemistry. III. The Role of Exact Exchange. *J. Chem. Phys.* **1993**, *98* (7), 5648–5652. https://doi.org/10.1063/1.464913.

(109) Burke, K.; Perdew, J. P.; Wang, Y. Recent Progress and New Directions. *Electron. Density Funct. Theory* **1998**, 81–111.

(110) Maron, L.; Eisenstein, O. Do f Electrons Play a Role in the Lanthanide-Ligand Bonds? A DFT Study of Ln(NR2)3; R = H, SiH3. *J. Phys. Chem. A* **2000**, *104* (30), 7140–7143. https://doi.org/10.1021/jp0010278.

(111) Maron, L.; Eisenstein, O. DFT Study of H - H Activation by Cp2 LnH D0 Complexes. *J. Am. Chem. Soc.* **2001**, *123* (6), 1036–1039. https://doi.org/10.1021/ja0033483.

(112) Maron, L.; Eisenstein, O.; Alary, F.; Poteau, R. Modeling C5H5 with Atoms or Effective Group Potential in Lanthanide Complexes: Isolobality Not the Determining Factor. *J. Phys. Chem. A* **2002**, *106* (9), 1797–1801. https://doi.org/10.1021/jp013693u.

(113) Booth, C. H.; Kazhdan, D.; Werkema, E. L.; Walter, M. D.; Lukens, W. W.; Bauer, E. D.; Hu, Y.-J.; Maron, L.; Eisenstein, O.; Head-Gordon, M.; Andersen, R. A. Intermediate-Valence Tautomerism in Decamethylytterbocene Complexes of Methyl-Substituted Bipyridines. *J. Am. Chem. Soc.* **2010**, *132* (49), 17537–17549. https://doi.org/10.1021/ja106902s.

(114) Booth, C. H.; Walter, M. D.; Kazhdan, D.; Hu, Y. J.; Lukens, W. W.; Bauer, E. D.; Maron, L.; Eisenstein, O.; Andersen, R. A. Decamethylytterbocene Complexes of Bipyridines and Diazabutadienes: Multiconfigurational Ground States and Open-Shell Singlet Formation. *J. Am. Chem. Soc.* **2009**, *131* (18), 6480–6491. https://doi.org/10.1021/ja809624w.

(115) Vitova, T.; Roesky, P. W.; Dehnen, S. Open Questions on Bonding Involving Lanthanide Atoms. *Commun. Chem.* **2022**, *5* (1), 1–4. https://doi.org/10.1038/s42004-022-00630-6.

(116) Pace, K. A.; Klepov, V. V.; Berseneva, A. A.; zur Loye, H. C. Covalency in Actinide Compounds. *Chem. - A Eur. J.* **2021**, *27* (19), 5835–5841. https://doi.org/10.1002/chem.202004632.

(117) Lohrey, T. D.; Bergman, R. G.; Arnold, J. Controlling Dinitrogen Functionalization at Rhenium through Alkali Metal Ion Pairing. *Dalt. Trans.* **2019**, *48* (48), 17936–17944. https://doi.org/10.1039/c9dt04489b.

(118) Ouellette, E. T.; Carpentier, A.; Joseph Brackbill, I.; Lohrey, T. D.; Douair, I.; Maron, L.; Bergman, R. G.; Arnold, J. σ or π? Bonding Interactions in a Series of Rhenium Metallotetrylenes. *Dalt. Trans.* **2021**, *50* (6), 2083–2092. https://doi.org/10.1039/d1dt00129a.

(119) Ouellette, E. T.; Magdalenski, J. S.; Bergman, R. G.; Arnold, J. Heterobimetallic-Mediated Dinitrogen Functionalization: N-C Bond Formation at Rhenium-Group 9 Diazenido Complexes. *Inorg. Chem.* **2022**, *61* (40), 16064–16071. https://doi.org/10.1021/acs.inorgchem.2c02463.

(120) Ryan, A. J.; Balasubramani, S. ganesh; Ziller, J. W.; Furche, F.; Evans, W. J. Formation of the End-on Bound Lanthanide Dinitrogen Complexes [(R2N)3Ln-N≠N-Ln(NR2)3]2-from Divalent [(R2N)3Ln]1-Salts (R = SiMe3). *J. Am. Chem. Soc.* **2020**, *142* (20), 9302–9313.

https://doi.org/10.1021/jacs.0c01021.

(121) Chung, A. B.; Rappoport, D.; Ziller, J. W.; Cramer, R. E.; Furche, F.; Evans, W. J. Solid-State End-On to Side-On Isomerization of (N═N)2-in {[(R2N)3Nd]2N2}2-(R = SiMe3) Connects In Situ LnIII(NR2)3/K and Isolated [LnII(NR2)3]1-Dinitrogen Reduction. *J. Am. Chem. Soc.* **2022**, *144* (37), 17064–17074. https://doi.org/10.1021/jacs.2c06716.

(122) Evans, W. J.; Lee, D. S. Early Developments in Lanthanide-Based Dinitrogen Reduction Chemistry. *Can. J. Chem.* **2005**, *83* (4), 375–384. https://doi.org/10.1139/v05-014.

(123) Gardiner, M. G.; Stringer, D. N. Dinitrogen and Related Chemistry of the Lanthanides: A Review of the Reductive Capture of Dinitrogen, as Well as Mono- and Di-Aza Containing Ligand Chemistry of Relevance to Known and Postulated Metal Mediated Dinitrogen Derivatives. *Materials (Basel).* **2010**, *3* (2), 841–862. https://doi.org/10.3390/ma3020841.

(124) Mondal, A.; Price, C. G. T.; Tang, J.; Layfield, R. A. Targeted Synthesis of End-On Dinitrogen-Bridged Lanthanide Metallocenes and Their Reactivity as Divalent Synthons. *J. Am. Chem. Soc.* **2023**, *145* (36), 20121–20131. https://doi.org/10.1021/jacs.3c07600.

(125) Ouellette, E. T.; Magdalenski, J. S.; Bergman, R. G.; Arnold, J. Applications of Low-Valent Transition Metalates: Development of a Reactive Noncarbonyl Rhenium(I) Anion. *Acc. Chem. Res.* **2022**, *55* (5).

(126) Jiang, S. Da; Liu, S. S.; Zhou, L. N.; Wang, B. W.; Wang, Z. M.; Gao, S. Series of Lanthanide Organometallic Single-Ion Magnets. *Inorg. Chem.* **2012**, *51* (5), 3079–3087. https://doi.org/10.1021/ic202511n.

(127) Chen, S. M.; Xiong, J.; Zhang, Y. Q.; Yuan, Q.; Wang, B. W.; Gao, S. A Soft Phosphorus Atom to "Harden" an Erbium(Iii) Single-Ion Magnet. *Chem. Sci.* **2018**, *9* (38), 7540–7545. https://doi.org/10.1039/c8sc01626g.

(128) Brennan, J. G.; Andersen, R. A.; Zalkin, A. Chemistry of Trivalent Uranium Metallocenes: Electron-Transfer Reactions with Carbon Disulfide. Formation of [(RC5H4)3U]2[M= H1, H2-CS2]. *Inorg. Chem.* **1986**, *25* (11), 1756–1760. https://doi.org/10.1021/ic00231a007.

(129) Minasian, S. G.; Krinsky, J. L.; Rinehart, J. D.; Copping, R.; Tyliszczak, T.; Janousch, M.; Shuh, D. K.; Arnold, J. A Comparison of 4f vs 5f Metal-Metal Bonds in Synthesis , Thermodynamics , Magnetism , and Electronic Structure. *J. Am. Chem. Soc.* **2009**, *131* (5), 13767–13783. https://doi.org/10.1021/JA904565J/SUPPL_FILE/JA904565J_SI_005.PDF.

(130) Brackbill, I. J.; Douair, I.; Lussier, D. J.; Boreen, M. A.; Maron, L.; Arnold, J. Synthesis and Structure of Uranium-Silylene Complexes. *Chem. - A Eur. J.* **2020**, *26* (11), 2360–2364. https://doi.org/10.1002/chem.202000214.

(131) Huber, K. P.; Herzberg, G. *Molecular Spectra and Molecular Structure*; Springer US, 1979. https://doi.org/10.1007/978-1-4757-0961-2.

(132) Irikura, K. K. Experimental Vibrational Zero-Point Energies: Diatomic Molecules. *J. Phys. Chem. Ref. Data* **2007**, *36* (2), 389–397. https://doi.org/10.1063/1.2436891.

(133) Odom, A. L.; Arnold, P. L.; Cummins, C. C. *Heterodinuclear Uranium/Molybdenum Dinitrogen Complexes [16]*; American Chemical Society , 1998; Vol. 120, pp 5836–5837.

(134) Lu, E.; Atkinson, B. E.; Wooles, A. J.; Boronski, J. T.; Doyle, L. R.; Tuna, F.; Cryer, J. D.; Cobb, P. J.; Vitorica-Yrezabal, I. J.; Whitehead, G. F. S.; Kaltsoyannis, N.; Liddle, S. T. Back-Bonding between an Electron-Poor, High-Oxidation-State Metal and Poor π-Acceptor Ligand in a

Uranium(v)–Dinitrogen Complex. *Nat. Chem.* **2019**, *11* (9), 806–811. https://doi.org/10.1038/s41557-019-0306-x.

(135) Evans, W. J.; Kozimor, S. A.; Ziller, J. W. A Monometallic f Element Complex of Dinitrogen: (C5Me 5)3U(H1-N2). *J. Am. Chem. Soc.* **2003**, *125* (47), 14264–14265. https://doi.org/10.1021/ja037647e.

(136) While it would have been ideal to use a completely non-coordinating solvent for these reactions, the insolubility of Na[Re(η^5-Cp)(BDI)] in any such solvents precluded that approach. Thus, we chose Et_2O as a less favorable L-type coordinating ligand relative to THF.

TOC

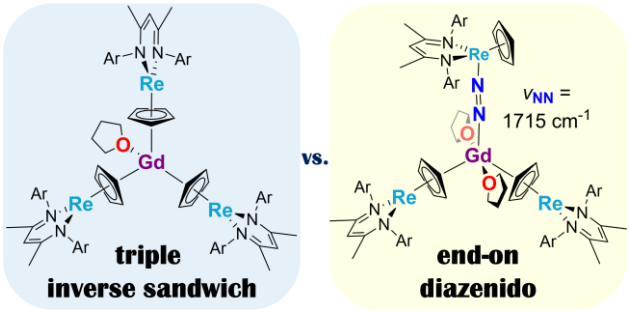

Synopsis: Salt elimination reactions between a rhenium metalate and lanthanide(III) salts lead to the synthesis of a series of triple inverse sandwich complexes for the early lanthanides. However, unexpected reactivity for gadolinium leads to structural characterization of both a triple inverse sandwich complex as well as an end-on/end-on heterobimetallic diazenido complex. We observe evidence for end-on diazenido formation with other heavy lanthanides as well as with uranium(III).